STRESS CONCENTRATIONS OF TENSILE STRIPS WITH
LARGE HOLES BY BOUNDARY ELEMENT TECHNIQUE

Dr. Galal A. Abdellah   Dr. Mohamed H. Abdalla
Faculty of Engineering   Faculty of Engineering
El-Mansoura University   Cairo University
El-Mansoura, Egypt.   Cairo, Egypt.

خـلاصـه : الحدود القصوى لمعامل تركيز الاجهادات عند الفتحات الدائريه في الشرائح المعدنيه المعرضه لشد سبق دراستها
من كثير من الباحثين . في هذا البحث يتم دراسه هذا التركيز باستخدام طريقه عناصر الحواف ومقارنته بالطرق السابقه لنسب
مختلفه من قطر الفتحه الدائريه / عرض الشريحه .

ABSTRACT: The limiting value of the stress-concentration factor at the edge of a large hole in a tensile strip as the hole diameter, a, approaches the strip width, w , has been investigated by many researchers. They made use of several theoretical, experimental and numerical techniques. There are two different solutions for the value of the stress concentration factor based on the net stress, k_{tn}. They are: k_{tn} = 1 and k_{tn} = 2. For this paper, the problem is analyzed by the boundary element method. A complete set of models with a/w = 0.4-0.99 is analyzed. The results indicate that the stress concentration factor is near two.

INTRODUCTION

The problem of determining the limiting value of the stress concentration factor in a tensile strip with a large central hole, as the hole diameter approaches the strip width, has attracted the interest of many researchers. Theoretical, experimental and numerical techniques (1-13) were applied to investigate the problem. It is interesting to note that a very good agreement is observed between the results of these studies up to the value of a/w = 0.6, where w is the strip width and, a, is the hole diameter. On the other hand, as a/w increases beyond 0.6 up to 1, the agreement ended and the limiting value of the stress concentration factor as a/w approaches one varies between one and two.

Enormous difficulties have faced the experimental modelling of the strip because of the narrowness of the strip at the minimum section, such as edge effects, imperfections in fabrication of the model, large deformations effects, etc. The boundary element technique can model the strip more efficiently than any other domain techinque. Due to symmetry of the strip only one quarter of the strip is considered with the necessary boundary conditions as illustrated in Figure (1). Two dimensional elastic analyses by using the boundary element method with different a/w ratio ranging between 0.3 and 0.99 are carried out. The results are presented and analysed. Conclusions are presented.

THE STRESS CONCENTRATION FACTOR-DEFINITIONS

Two types of stress concentration factor are used in the literature dealing with plates having holes as shown in Figure (1). They are:

$$k_{tg} = \frac{q_{max}}{\sigma} \quad \dots\dots\dots\dots\dots\dots\dots\dots\dots\dots\dots\dots\dots\dots\dots\dots (1)$$

$$\text{and } k_{tn} = \frac{q_{max}}{\sigma_{nom}} \quad \dots\dots\dots\dots\dots\dots\dots\dots\dots\dots\dots\dots\dots\dots (2)$$

where:

k_{tg} = stress concentration factor based on gross stress.

σ_{max} = maximum stress at edge of the hole.

σ = applied stress, distant from hole.

k_{tn} = stress concentration factor based on net (nominal) stress.

σ_{nom} = nominal (net) stress.

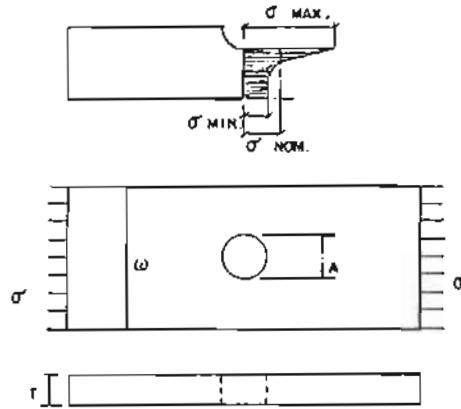$$\sigma'/\sigma_{nom} = (1 - \frac{a}{\omega}) \dots\dots\dots (3)$$

FIG. I SCHEMATIC OF THE TENSILE STRIP WITH CENTRAL HOLE.

Combining (1) & (2) and (3) one gets

$$K_{tn} = K_{tg} (1 - \frac{a}{\omega}) \dots\dots (4)$$

$$K_{tn} = \frac{\sigma_{max}}{\sigma} (1 - \frac{a}{\omega}) \dots\dots (5)$$

Similarly, a factor K_{tn} min which relates the minmum stress to applied stress can be defined as :

$$K_{tn\ min} = \frac{\sigma_{min}}{\sigma} (1 - \frac{a}{\omega}) \dots\dots (6)$$

Reference in this paper is made to both K_{tn} and $K_{tn\ min}$.

LITERATURE REVIEW

As mentioned earlier, three different approaches have been used to investigate the problem of circular hole in a thin plate. They are : theoretical, experimental, and numenical techniques.

THEORETICAL ANALYSIS

The case of a circular hole in an infinite plate was solved by

Kirsch [1]. He concluded that the stress concentration factor equals 3.
Howland [2] has applied a series solution for the cases of $\frac{a}{\omega}$ up to 0.5
to obtain K_{tn}. Howland results were used later to calibrate most of the
experimental results as well as the numerical techniques results. Timos-
henko [3], treated the problem theoretically and concluded that for the
case of infinite plate with stress applying at the ends stress concent-
ration factor is equal to 3 .

EXPERIMENTAL ANALYSIS

Two main experimental techniques were used to investigate the
problem, i.e., photoelastic analysis and testing of a steel model and
analysing the measured strains.

The results of the photoelastic analysis are again not in agreement.
Coker and Filon [4], noted that as $\frac{a}{\omega}$ approaches one, the stress concen-
tration factor approaches 2. The same result is obtained by Wahl and
Beeuwkes [5], Koiter [6] and Heywood [7]. On the other hand, Hennig's
results indicated a trend towards a limiting value equal to one [8].
Wahl and Beeuwkees [5] noting the difficulty in investigating this "thin
ligament" region photoelastically, made a steel model 4.125 in-wide with
a 4 in-diameter circular hole ($\frac{a}{\omega}$ = 0.97). By means of strain measurments
they obtained K_t = 1.92, but they believed that for very small deformations
the K_t value would be higher. They stated that "in case the hole diameter
so closely approaches the width of the bar that the minimum section becomes
an infinitely thin filament, then for any finite deformation, this filament
may move inward sufficiently to allow for a uniform stress distribution,
thus giving K_t = 1. For infinitely small deformations relative to the
thickness of this filament, however, K_t may still be equal to 2. They not-
ed that the steel model test indicated that the curve does not drop down
to unity as fast as would appear from certain photoelastic tests.

They noted that the difference between σ/E for steel model and ($\frac{\sigma}{E}$)
for photoelastic model is quite large which affected the magnitude of the
inward movement. This caused that K_t would not drop to one for the steel
model.

Belie and Appl [9] empolyed a singular integral method of numerical
analysis of plane-elasticity problems to obtain an approximate elasticity
solutions for the problem. The method was a stress-boundary-value coll-
ocation method in which equilibrium and compatibility conditions are satis-
fied at discrete points around the boundary. Using this technique and
photoelastic analysis for $\frac{a}{\omega}$ ranging between 0.1 & 0.99 they concluded that
K_{tn} approaches one as the ratio for a/ω approaches a value of one.

Riesen and Spiering [10] applied a point-matching technique which
combines the collocation method with the method of least squares to obtain
the numerical solution for stresses and displacements of plane elastostatic
problems. The technique satisfies the equilibrium and compatibility cond-
itions in the region by a number of functions, each is multiplied by an
unknown coefficient. The techinque enabled them to compute the stress
distribution in inter-boundary and interior points which made it possible
for them to check the assumption made by Koiter of a linear stress distrib-
ution through the height of the ligament when $\frac{a}{\omega}$ approaches one.

They concluded that the Koiter's assumption is admissible. Also, they perferredphotoelastic analysis of the problem. Their conclusion was that the stress concentration factor tends to two when a/w tends to one. On the contrary Parks and Mendoza [11], after conducting a photoelastic investigation have concluded that the limiting value of K_{nt} is two.

NUMERICAL ANALYSIS

As stated earlier, different numerical techniques have been used to investigate the limiting value of K_{tn}. These include the approximate elasticity solutions adopted by Belie and Appl [9] and a point matching technique used by Riesen and Spiering [10].

The Finite elements technique was first used by Fuehring [12] to obtain K_{tn} for the limiting case of tensile strip with circular hole. Fuehring empolyed a mesh generating program which enabled him to adjust the mesh and speed up the convergence of the results. Fuehring concluded that K_{tn} tends' to two as $\frac{a}{w}$ tends to one.

Chong and Pinter [13] have applied the finite element method to investigate the limiting case. They employed two dimensional rectangular elements. Seven models with different $\frac{a}{w}$ ratios were studied with the length of the strip kept at a minimum of seven times the hole diameter in order to ensure that a constant stress field would develop outside the stress field produced around the hole. They noted that the accuracy of the finite element method is a function of the mesh density of the models used. They noted a strong tendency for a limiting value of K_{tn} that is less than two, but not approaching one and they concluded that K_{tn} tends to 1.63 as $\frac{a}{w}$ tends to 1.

To the authors best knowledge, the boundary element technique has not been applied to this problem before.

THE BOUNDARY ELEMENT TECHNIQUE

The boundary element method (BEM) is based upon classical integral equation formulation of the boundary value problems. The (BEM) has been developed recently to the extent it becomes a powerful general purpose procedure for obtaining numerical results to many engineering problems. The full formulation of the two dimensional linearly elastic problem can be found in several references [14, 15]. However, a brief development is presented next for the sake of completeness.

The 2D domain Ω illustrated in Fig. (2) is bounded by the boundary Γ with mixed boundary conditions, i.e., the part Γ_1, of the boundary has prescribed displacement boundary conditions while on the remaining.
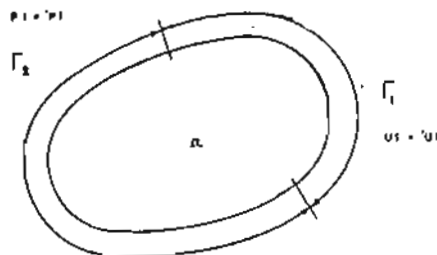

FIGURE (2) Domain Ω

portion of the boundary   traction boundary conditions are prescribed.
The displacement constraint are

$$u_i = \bar{u}_i \qquad\qquad \text{on } \Gamma_1 \qquad \ldots\ldots\ldots\ldots\ldots (7 - a)$$

and the traction conditions are

$$P_i = \sigma_{ji} \, n_j = \bar{p}_i \qquad \text{on } \Gamma_2 \qquad \ldots\ldots\ldots\ldots\ldots (7 - b)$$

where

$\quad n_j \quad$ is the out-ward normal to the boundary.

$\quad \bar{P} \quad$ the prescribed tractions on $\quad \Gamma_2$

$\quad \bar{u} \quad$ the prescribed displacement on Γ_1

and $\qquad \Gamma = \Gamma_1 + \Gamma_2 \qquad\qquad \ldots\ldots\ldots\ldots\ldots (7 - c)$

The reciprocal work theorem can be stated as follows:If two distinct
elastic equilibriun states (b_i^*, t_i^*, u_i^*), (b_i, t_i, u_i) exist
in the region Ω bounded by the surface Γ then the work done by the forces
of the first system (*) on the displacements of the second is equal to
the work done by the forces of the second system on the displacements of
the first (*). Thus

$$\int_\Gamma t_i^*(P)\, u_i(P)\, ds\,(P) + \int_\Omega b_i^*(Z)\, u_i(Z)\, d\Omega\,(Z) =$$

$$\int_\Gamma t_i(P)\, u_i^*(P)\, ds\,(P) + \int_\Omega b_i(Z)\, u_i^*(Z)\, d\Omega\,(Z) \qquad \ldots\ldots\ldots\ldots (8)$$

where P is a point on Γ and Z is a point in Ω. If the actual state of
displacements, tractions and body forces is chosen as (u_i, t_i, b_i) and
the (*) system as those corresponding to a unit force at point S in the
direction t_i^* (P) and u_i^* (P) , and making use of the following relations
(14).

$$t_i^* \ (P) = T_{ij}^* \ (p,s)\, n_i \ (S) \qquad \ldots\ldots\ldots\ldots (9 - a)$$

$$u_i^* \ (P) = G_{ij}^* \ (p,s)\, n_i^* \ (S) \qquad \ldots\ldots\ldots\ldots (9 - b)$$

$$b_i^* \ (Z) = e_i^* \ (Z) \qquad\qquad \ldots\ldots\ldots\ldots (9 - c)$$

one obtains

$$\int_\Gamma T_{ij}^* \ (p,s)\, u_i \ (p)\, d\Gamma \ (p) + \int_\Omega \sigma_{ij} \, \sigma(Z, p)\, ui \ (Z)\, dV \ (Z)$$

$$= \int_\Gamma t_i \ (S) \ G_{ij}^* \ (s,p)\, d\Gamma \ (S) + \int_\Omega b_i(Z)\, G_{ij}^* \ (z, p) \ d\Omega \ (Z) \ldots (10\text{-}a)$$

The second term in the left hand side can be simplified as $\beta\, u_i(P)$ where $\beta = 1$ in the domain and $= 0$ outside the domain .

The eqn. can be written as :

$$u_j (P) = \int_\Gamma [\ t_i(P)\ G_{ij}^* (P,S) - T_{ij}^* (P,s)\ u_i(s)]$$

$$dS\ (P)\ +\ \int_\Omega b_i(Z)\ G_{ij}^* (P,S)\ d\Omega (s) \quad \dots\dots\dots\dots (10 - b)$$

By bringing point P to the boundary $\beta \sim -\frac{1}{2}$ [14]. The eqn. becomes.

$$\tfrac{1}{2}\, u_j (S) = \int_\Gamma [t_i (S)\ G_{ij}^* (p,s)\ - T_{ij}^* (p,s)\ u_i(p)]$$

$$d\Gamma (S)\ +\ \int_\Omega b_i(\Omega)\ d\Omega \quad \dots\dots\dots\dots\dots (11 - a)$$

where :-

$$T_{ij}^* (p,s) = \frac{-1}{4\ \Pi\ (1-\nu)\ r} \{\ \frac{\partial r}{\partial n} \{(1-2\nu)\delta_{ij} + 2r,_i\, r,_j\}$$

$$- (1-2\nu)(r,_i\ n_j - r,_j\ n_i)\ ] \quad \dots\dots\dots\dots\dots (11 - b)$$

$$G_{ij}^* (P,S) = \frac{1}{16\ \pi(1-\nu)\,Gr} \quad (3-4\nu)\delta_{ij} + r,_i\ \ r,_j) \dots\dots\dots (11 - c)$$

$$e_i \qquad = \text{unit vector in direction } i . \qquad \dots\dots\dots (11 - d)$$

$$\frac{\partial r}{\partial n} = r,_i\ n_i, \qquad \dots\dots\dots\dots\dots (11 - e)$$

$$r = (r_i\ r_i)^{\tfrac{1}{2}}, \qquad \dots\dots\dots\dots\dots (11 - f)$$

$$r_i = x_i (q) - x_i(S), \qquad \dots\dots\dots\dots\dots (11 - g)$$

$$r,_i = \frac{\partial r}{\partial x_i} (q)\ = \frac{r_i}{r} \qquad \dots\dots\dots\dots\dots (11 - h)$$

Equation (11) is the starting equation for the boundary element technique.

BOUNDARY ELEMENT DISCRETIZATION

Neglecting the effect of body forces, equation (11-a) for the two dimensional case with the point "S" as a boundary point on a smooth boundary becomes,

$$\tfrac{1}{2} u_i (S) + \int_{\Gamma} u_j (q) P_{ij}^* (S,q) \, d\Gamma =$$

$$\int_{\Gamma} P_j(q) \, u_{ij}^* (S,q) \, d\Gamma , \qquad i=1,2 \dots\dots\dots\dots\dots (12)$$

In order to evaluate the integral contained in equation (12), it is assumed that the boundary of the domain Ω is divided into N boundary elements as shown in Fig.(3) . Using the constant element method, the nodes are taken to be at the middle of each element. The tractions and displacements are assumed to be constant allover the straight element of the boundary.

Hence equation (12) becomes :

$$\tfrac{1}{2} u_i (S) + \sum_{q=1}^{N} u_j^q \int_{\Gamma_q} P_{ij}^* (S,q) \, d\Gamma_{(q)} =$$

$$\sum_{q=1}^{N} P_j^q \int_{\Gamma_q} u_{ij}^* (S,q) \, d\Gamma_{(q)} \qquad i=1,2 \dots\dots\dots\dots (13)$$

In which,

N   is the number of boundary elements (total number of nodes).

Γ_q denotes the surface of the qth boundary element.

u_j^q and P_j^q are the values of the displacements and tractions respectively in the direction "J" at point "q".

s $= 1, 2, 3, \dots\dots\dots\dots$ N boundary segments.

Adopting the following definitions.

$$\hat{H}_{ij} = \int_{\Gamma_j} P^* \, d\Gamma \qquad \dots\dots\dots\dots\dots\dots\dots\dots (14)$$

and $G_{ij} = \int_{\Gamma_j} u^* \, d\Gamma \qquad \dots\dots\dots\dots\dots\dots\dots\dots (15)$

Equation (13) reduces to the following form :

$$c^i u^i + \sum_{j=1}^{N} \hat{H}_{ij} u_j = \sum_{j=1}^{N} G_{ij} P_j \dots\dots\dots\dots\dots\dots (16)$$

This equation relates the value of u at midnode "i" with the values of u's and p's at all the nodes on the boundary, including i.

Define further,

$$H_{ij} = \hat{H}_{ij} \qquad \text{in case } i \neq j \dots\dots\dots\dots\dots (17)$$

$$H_{ij} = \hat{H}_{ij} + c^i \qquad \text{in case } i = j \dots\dots\dots\dots\dots (18)$$

Hence, equation (16) becomes,

$$\sum_{j=1}^{N} H_{ij} u_j = \sum_{j=1}^{N} G_{ij} p_j \quad \dots \dots \dots \dots \dots \dots (19)$$

The integrals for H_{ij} and G_{ij} can be calculated using the 4-point Gauss quadrature formula.

SYSTEM OF EQUATIONS

Numerical evaluation of eqn. (19) will produce a system of equations for the node under consideration. Repeating for all the nodes gives a final system of equations that can be written as

$$HU = GP \quad \dots \dots \dots \dots \dots \dots (20)$$

in which U are the displacements; P are the values that the distributed tractions take at all the boundary nodes.

It is important to point out that the diagonal coefficients in the H matrix can be obtained by applying rigid body condition. If unit rigid body displacements are assumed in all directions, eqn. (20) becomes.

$$HU_r = 0 \quad \dots \dots \dots \dots \dots \dots (21)$$

Thus, the submatrices, or the diagonal, of H can be determined. Note that if M values of displacements and $N - M$ values of tractions are known, therefore, one has a set of N unknowns in equation (20). Reordering the equations, i.e., with the unknowns on the left-hand side vector X, we obtain.

$$AX = F \quad \dots \dots \dots \dots \dots \dots (22)$$

ANALYSIS AND RESULTS

As mentioned earlier, the boundary element analysis of the problem of a tensile strip with large hole was carried out for one quarter of the strip only because of symmetry. Fig. (3) illustrates a typical boundary element mesh for the strip. The constant element is used in which both the traction and displacement are uniformlly distributed over the element. Two points are worth noting in this typical mesh. They are, (1) the length of the mesh is taken at least ten times the width of the strip to ensure the uniformity of the stress field away from the hole, (2) the size of the elements is decreased at the region of the minimum section and subsequently the number of elements is increased in the region in order to improve the accuracy of representing the rapidly changing stress field near the minimum section. The boundary elements are needed only on the boundary, fewer elements are needed to model the strip than those needed to model it by the finite element where the domain is divided into elements. This enables one to use finer boundary element mesh in order to achiéve better results.

The main objective of this study is to determine the stress concentration factor for the limiting case as $\frac{a}{w}$ approaches one for the strip with central hole. Two dimensional plane stress analyses by the boundary element technique is carried out. Several models with different $\frac{a}{w}$ ratios ranging between 0.3 and 0.99 are studied under the action of direct tension. The results are reported and analysed below.

Fig (4) shows the typical stress distribution over the minimum section for the case of $\frac{a}{\omega} = 0.4$. In table (1) the resulting K_{tn} values obtained in the present study is compared with those reported by Chang [13]. It can be observed from table (1) that K_{tn} values obtained by the boundary element agreed very well with other results up to $\frac{a}{\omega} = 0.7$. It is observed that the stress distribution across the minimum section is non linear up to $\frac{a}{\omega} = 0.7$ with a very distinctive shape made up of decreasing and increasing slopes. However, a tendency of the stress distribution to become linear appears as $\frac{a}{\omega}$ increases. As $\frac{a}{\omega}$ increases beyond 0.9, fluctuation of the stresses is observed in the middle part of the minimum cross section while the outer part becomes flatter and tends to be linear. At $a/\omega = 0.99$, the slopes of the stress distribution curves at both the outer edge and the hole edge are very close to each other and almost linear as shown in Fig (5). This stress distribution is similar to that of the pure bending case. It also confirms the results reported by Appl [9] and Chang [13].

Fig. (6) illustrates the deformed shape of the strip for the case of $\frac{a}{\omega} = 0.99$. It is interesting to note that the vertical deformation across the minimum section is quite large and it seems to be that considering only the small deformations provides non realistic representation of the problem. The general deformed shape of the strip shown in Fig. (6) is similar to that obtain by the finite element method and reported by Fuehring [12].

The stress distribution at $\frac{a}{\omega} = 0.99$ indicates a value of $K_{tn\ max}$ equal to 2.23. Fig. (7) illustrates the K_{tn} values for different a/ω values obtained in the present work and those obtained by other reseachers. It can be predicted from Fig. (7) that K_{tn} is decreasing as $\frac{a}{\omega}$ increases from 0.99 to 1. It seems to be reasonable to conclude that K_{tn} is approaching 2 as a/ω approaches one .

CONCLUSION

The boundary element analyses of the strip with large central hole reported here justifies the conclusion that K_{tn} is tending to the value of two as a/ω is tending to one. It is also evident that a more accurate stress concentration value can be obtained if the non linearity of both the geometery and materials is considered .

Table (1)　Comparsion of Results obtained by boundary elements and Finite elememts .

$\dfrac{a}{\omega}$	Present Study Boundary element analyses		Chang & Pinter Finite element analyses	
	K_{tn}	$K_{tn\,min}$	K_{tn}	$K_{tn\,min}$
0.3	2.135	0.64	2.41	0.65
0.4	2.13	0.51	2.30	0.53
0.5	2.25	0.458	2.21	0.458
0.6	3.20	0.266	N.A	N.A
0.7	2.30	0.35	2.15	0.29
0.8	1.33	0.35	2.06	0.28
0.9	1.99	0.566	1.95	0.31
0.99	2.25	0.58	1.63	0.59
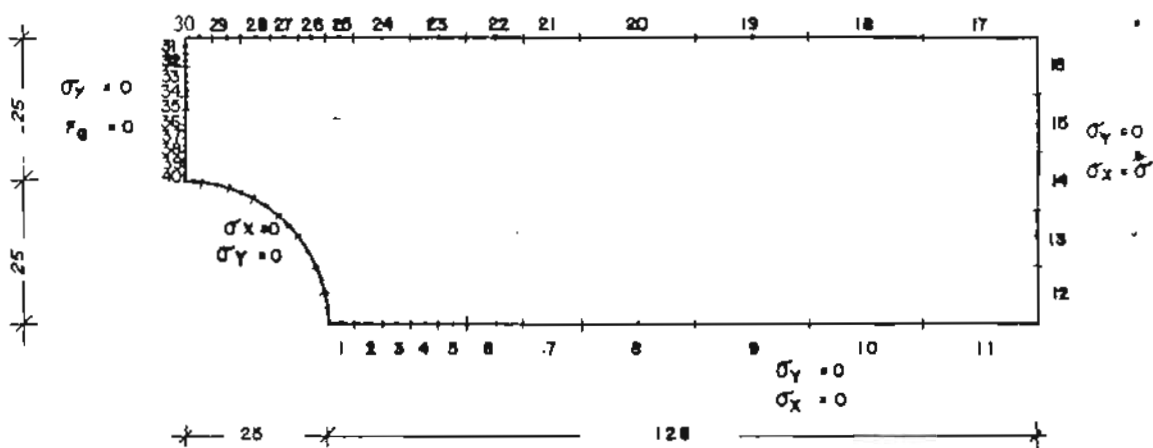
FIG 3　BOUNDARY ELEMENT MESH FOR THE TENSILE STRIP FOR A/W 0.9
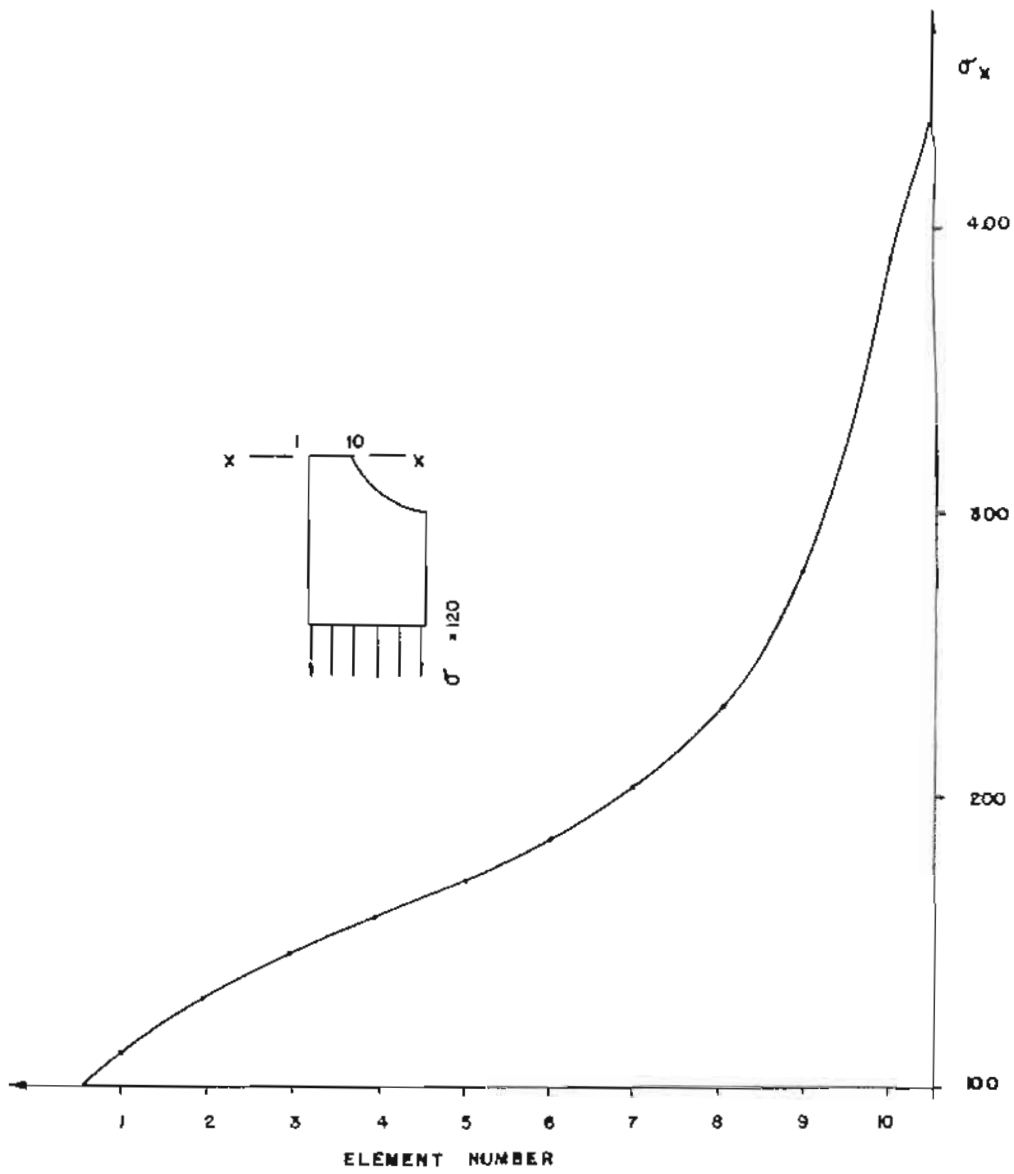
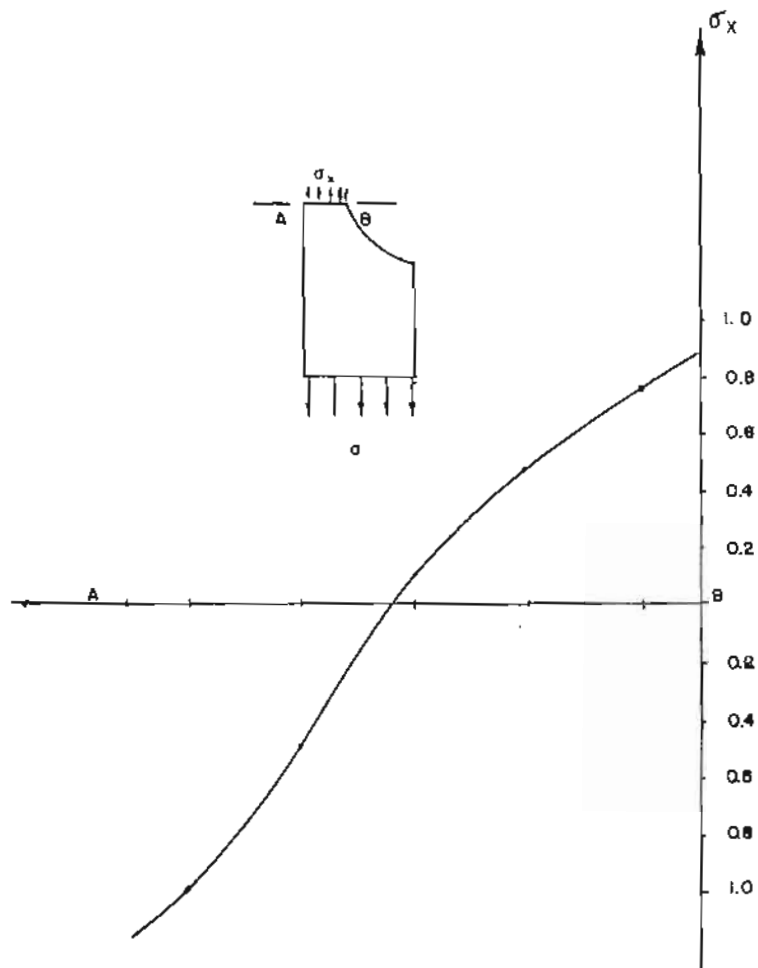FIG 4 STRESS DISTRIBUTION ACROSS THE MINIMUM SECTION   A/W=0.4

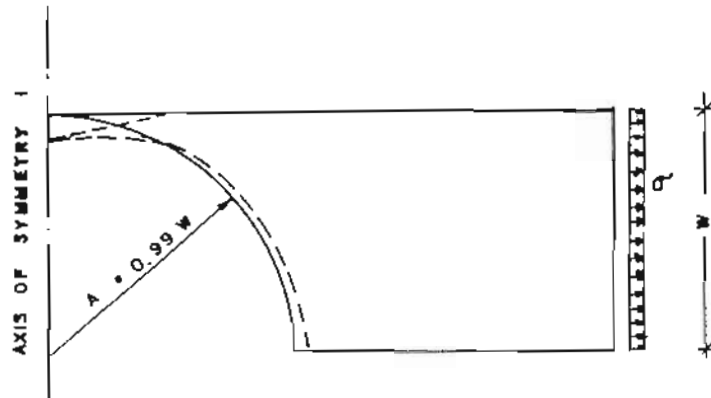FIG 5 STRESS DISTRIBUTION ON THE MINIMUM SECTION
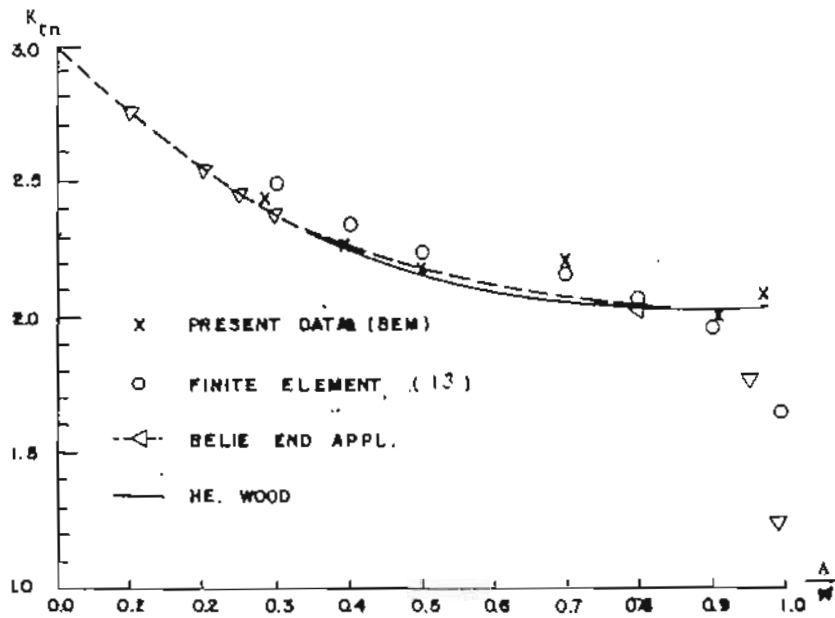
FOR A/W ±0,99

FIG (6) DEFORMED SHAPE FOR A/W = 0.99

FIG (7) STRESS CONCENTRATION FACTORS FOR A/W TENSILE
STRIPS CONTAINING A CIRCULER HOLE

C. 89 Galal A.Abdellah & Mohamed H.Abdalla .

REFERENCES

1. Kirsch, G. "Die Theorie der Elastizitat und die Beduerfnisses der Festigkeitslehre", Zeitschrift des Vereines Duetscher Ingenieure, 42, 797 (1898).

2. Howland R.C., "On the Stresses in the Neighborhood of a Circular Hole in a Strip Under Tension", Philosophical Transactions of the Royal Society (London) Ser. A, 229, 49 (1929 - 1930).

3. S.P. Timoshenko and J.N. Goodier, " Theory of Elasticity", 2nd Edn, PP. 78-85. Mc. Graw-Hill. New York (1951).

4. R.E. Peterson, "Stress Concentration Factors", PP. 108-111, 150 Willey, New York, 1972.

5. Wahl, A.M. and Beeuwkes, Jr., R., "Stress Concentration Produced by by Holes and Notches", Trans. ASME, 56, 617 (1934).

6. Koiter, W.T., "An Elementary Solution of Two Stress Concentration Problems in the Neighbourhood of a Hole", Qtly. of Appl. Math., 15, 303 (1957).

7. Heywood, R.B., "Designing by Photoelasticity", 267-270, Chapman and Hall, Ltd., London (1952).

8. Hennig, A., "Polarisation - optische Spannungsuntersuchung am Gelochten Zurgstab und am Nietroch", Forschung auf dem Gebiete des Ingenieurwesens, 4(2), 53(1933).

9. R.G. Belie and F.J. Appl, "Stress Concentrations in Tensile Strips With Large Circular Holes". Experimental Mech. 13 (6), 256 (1973).

10. P.E. Van Riesen and R. M. E. M. Spiering, "Investigation of Stress-Concentration Factors in Tensile Strips". Experimental Mech. 15 (3), 111-113 (1975).

11. V.J. Parks and D.F. Mendoza, "Maximum Stress in a Tensile Strip With a Large Hole". Experimental Mech. 15 (10), 389-391 (1975).

12. H. Fuehring, Discussion of "Stress Concentations in Tensile Strip With Large Circular Holes", by R.G. Belie and F. J. Appl. Experimental Mech. 13 (6), 255-256 (1973).

13. Chang, K. P. and Pinter, W.J., "Stress Concentrations of Tensile Strips With Large Holes", Computers & Structure Vol. 19. No. 4, PP. 563-589, 1984.

14. Brebbia, C.A., "The Boundary Element Method for Engineers", Pentech Press, London 1978.

15. Banerjee, P.K., and Butterfield, R., "Developments in Boundary Element Method-1", Applied Science Publishers LTD, London 1979.